Two-State Model for the Photophysics of 9,9′-Bianthryl. Fluorescence, Transient-Absorption, and Semiempirical Studies†

Gottfried Grabner,*,‡ Karl Rechthaler,§ and Gottfried Köhler*,‖

Institut für Theoretische Chemie und Strahlenchemie, University of Vienna, Althanstrasse 14, A-1090 Wien, Austria

Received: August 26, 1997; In Final Form: November 13, 1997

The photophysics of 9,9′-bianthryl (BA) were investigated by means of fluorescence spectroscopy, nanosecond transient-absorption spectroscopy, and semiempirical calculations. Fluorescence spectra and lifetimes were measured in more than 50 solvents in order to get a detailed picture of the solvent dependence. The results show that the fluorescence lifetime is constant in solvents of low polarity ($D < 5$) and increases with solvent polarity in more polar solvents. Departures from this trend can be traced to specific solute−solvent interactions. Excited-state singlet−singlet absorption spectra were measured in the ultraviolet range and show a marked solvent dependence. In polar solvents, the spectrum ($\lambda_{max} = 315$ nm) is closely related to those of the radical ions of both BA and anthracene. The decay rate constant of this band is identical with that of the fluorescence emission in a range of solvents of varying polarity ($D > 5$), thus providing direct proof of the charge-separated character of the fluorescent state in polar solvents. The 315 nm band is absent in isooctane, indicating that the fluorescent state is not of charge-separated character in this case. Semiempirical calculations were carried out in order to rationalize the experimental data. Careful consideration of the symmetry character of the electronic states involved and of the solvent effect on these states indicates that two distinct transitions are responsible for the observed fluorescence emission; in nonpolar solvents, a nonpolar state with D_2 symmetry and a torsion angle that is markedly smaller than 90° is the fluorescent state, whereas in polar solvents fluorescence originates from a charge-separated perpendicular state of D_{2d} symmetry. This latter state is responsible for the large solvent effects on fluorescence and singlet−singlet absorption. Triplet−triplet absorption and intersystem-crossing efficiency data were also measured in several solvents. They too are solvent-dependent but do not show characteristics of charge separation; they rather are influenced by specific solute−solvent interactions.

1. Introduction

The phenomenon of dual fluorescence induced by polar solvents in aromatic bichromophoric systems, composed of two moieties with different redox properties and connected by a single bond, has been among the most intensely studied topics in photophysics during the past 2 decades.[1] The sequence of processes initiated by excitation is supposed to result in charge separation and to involve torsional motion about the single bond connecting both aromatic subunits. The final fluorescing state is thus often referred to as *twisted intramolecular charge transfer* or TICT state.[2,3] Charge separation in the relaxed fluorescent state is now widely accepted as the central cause of this effect, although diverging explanations, such as formation of probe−solvent exciplexes,[4] have also been advanced.

A similar relaxation mechanism was also proposed for some symmetric biaryls exhibiting strongly solvent-dependent emission properties. The appearance of a second, red-shifted fluorescence band was first observed for 9,9′-bianthryl (BA; see Scheme 1)[5,6] and is consistent with a large dipole moment in the excited state.[7] Subsequently, various experimental and theoretical methods have been applied to the study of this solvent-induced symmetry breaking.[8−18] In this respect, symmetric biaryls are reminiscent of the photosynthetic reaction center, and structural similarities have been pointed out.[19,20]

SCHEME 1

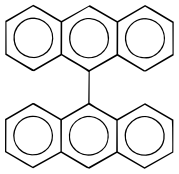

9,9'-Bianthryl (BA)

In the ground state of BA, the two anthracene moieties are considered to be orthogonal mainly because of steric hindrance and lack of electronic resonance between the two subunits. This is also manifested in the heat of formation of the compound, its molecular polarizability, and its polarographic half-reduction potential.[21−23] In the vertical nonpolar singlet excited state, an optimum torsion angle of about 70° was deduced from the vibronic structure of laser-induced fluorescence spectra of BA in a free jet[24−26] and from a simulation of steady-state and time-resolved fluorescence spectra in nonpolar solvents.[27] The relaxed nonperpendicular configuration facilitates electron transfer from one subunit to the other if the charge-separated state is additionally stabilized in a polar environment.[28] The perpendicular conformation should again be favored in the TICT

† This paper is dedicated to Zbigniew R. Grabowski on the occasion of his 70th birthday.

‡ Fax: 43-1-31336-790. E-mail: Gottfried.Grabner@univie.ac.at.
§ Fax: 43-1-31336-790. E-mail: karl.rechthaler@univie.ac.at.
‖ Fax: 43-1-31336-790. E-mail: Gottfried.Koehler@univie.ac.at.

S1089-5639(97)02781-3 CCC: $15.00
Published on Web 01/01/1998

state itself in order to minimize electronic overlap and to prevent back electron transfer. Further detailed studies of the solvent dependence of the fluorescence spectra and of the excited-state equilibirium between locally excited and charge-transfer states have been reported recently.[29−31]

The application of BA to probe solvation processes is based on the solvent dependence of the effective S_1 torsional potential and the resulting torsional dynamics.[32,33] Dynamic solvation effects show up in the time-resolved Stokes shift of the fluorescence spectra[32] on one hand and in variations of the $S_n \leftarrow S_1$ absorption spectrum in the visible spectral region[34−37] on the other. The picosecond transient-absorption spectra obtained in alkane solution show a peak around 575 nm and no significant change in time, but as the solvent becomes polar, a new band at 694 nm appears, which has been attributed to the charge-separated state by virtue of its similarity to the anthracene radical-ion absorption.[34] Triplet−triplet absorption spectra were obtained in the microsecond time domain, but their shape is not significantly dependent on solvent polarity.[34,38]

A conclusive proof of the charge-separation hypothesis requires a direct experimental demonstration of the charge-separated structure of the fluorescing state. The observation of a radical-ion spectrum among the transients cannot be regarded as definitive proof, since radical cation formation by (two-photon) photoionization in polar solvents can hardly be ruled out under the conditions of picosecond excitation. On the other hand, the inherent similarity of the absorption spectra of radical anions and radical cations may preclude the distinction among these species. A kinetic demonstration of the identity of the states measured in absorption and emission is therefore needed. A step in this direction was taken in measurements of the kinetics of the decay of the locally excited state and of the concomitant growing-in of the charge-separated state, again by picosecond transient absorption, of BA and derivatives of BA in 1-pentanol,[35] and of BA in glycerol triacetate as a function of pressure.[36] Although these results clearly identified the locally excited state as the precursor of the charge-separated state, thus precluding formation of the latter by a different mechanism, demonstration of the identity with the fluorescing state is still lacking.

In the present work, we have studied fluorescence properties in a wide variety of solvents with the aim of elucidating the main contributions to solvent effects on dual luminescence. Nanosecond transient-absorption spectroscopy was used to investigate $S_n \leftarrow S_1$ absorption and decay kinetics of BA in a series of solvents of varying polarity. The advantages of using this conventional technique for addressing the problem stated above lie (a) in easy accessibility of the UV region for transient-absorption measurement, (b) in easy distinction of one- and two-photon processes by measurements of photon-fluence dependence, and (c) in probing processes within the time scale of fluorescence decay. We further report measurements of the influence of solvent on intersystem-crossing quantum yields and on $T_n \leftarrow T_1$ absorption spectra of BA. These data are discussed in the context of the results of fluorescence spectroscopy. Additionally, semiempirical calculations have been performed on structural relaxation processes in the excited state, with explicit inclusion of the effects of solvent polarity. Taken together, the results give a consistent picture of the relaxation pattern involved in the excited-state decay of 9,9′-bianthryl.

2. Experimental Section

2.1. Synthesis of 9,9′-Bianthryl. 9,9′-Bianthryl was synthesized by reductive dimerization of anthrone.[39] The pale-yellow product was recrystallized twice from acetanhydride and washed with pentane. The melting point of the product was 589.4−591.5 K (IA9200, Electrothermal Eng.Lim.).

2.2. Solvents. The solvents were of the best available quality (the numbering of solvents used throughout the text is given in parentheses): isooctane (1), Merck Uvasol; benzene (2), Merck Uvasol; toluene (3), Merck p.a.; tetralin (4), Merck f.synthesis; carbon disulfide (5), Merck p.a.; thiophene (6), Merck f.synthesis; tetrachloromethane (7), Merck Uvasol; 1,2-dichloroethane (8), Merck puriss.; 1,1,1-trichloroethane (9), Merck p.a.; 1,2-dibromoethane (10), Merck f.synthesis; 1-chlorobutane (11), Aldrich HPLC-quality; chlorobenzene (12), Merck f.synthesis; bromobenzene (13), Fluka puriss.; iodobenzene (14), Fluka puriss.; ethyl ether (15), Merck Uvasol; *tert*-butyl methyl ether (16), Aldrich HPLC-quality; propyl ether (17), Aldrich 99+%; butyl ether (18), Fluka puriss.p.a.; tetrahydrofuran (19), Fluka for UV spectroscopy; acetone (20), Merck Uvasol; butanone (21), Fluka puriss.p.a.; cyclohexanone (22), Janssen 99.6%; diethylamine (23), Fluka puriss.p.a.; triethylamine (24), Merck f.synthesis; pyridine (25), Merck Uvasol; quinoline (26), Merck f.synthesis; acetonitrile (27), Merck Uvasol; propionitrile (28), Merck Aldrich 99%; benzonitrile (29), Merck f.synthesis; *N*,*N*-dimethylformamide (30), Merck Uvasol; *N*,*N*-dimethylacetamide (30), Merck f.synthesis; *N*-methyl-2-pyrrolidone (31), Loba p.a.; diethyl ethanephosphonate (32) from triethyl phosphite (Merck f.synthesis), traces of ethyl iodide and sodium iodide by Michaelis−Arbuzow reaction; dimethyl sulfoxide (33), Fluka puriss.p.a.; propylene carbonate (34), Merck f.synthesis; methanol (35), Donauchem HPLC; ethanol (36), Merck p.a.; 2,2,2-trifluoroethanol (37), Merck Uvasol; 1-propanol (38), Aldrich 99+% spectrophotometric grade; propanol-2 (39), Merck LiChrosolv; allyl alcohol (40), Merck f.synthesis; 1-butanol (41), Merck Uvasol; 2-butanol (42), Merck p.a.; 2-methyl-1-propanol (43), Merck p.a.; 2-methyl-2-propanol (44), Merck p.a.; 1-pentanol (45), Merck p.a.; cyclohexanol (46), Merck f.synthesis; benzyl alcohol (47), Merck p.a.

Each solvent was checked for absorbing and fluorescing impurities. Solvents less pure than p.a. quality were purified according to standard methods. Dielectric permittivity (D^{293}) and refractive index (n_D^{293}) data were taken from standard tables.[40] Solutions were purged with argon (Messer-Griesheim, 5.5) for several minutes in order to remove oxygen.

2.3. Apparatus. Absorption spectra were recorded on a Perkin-Elmer UV−vis Lambda 16 spectrophotometer. Measurements of fluorescence spectra and decay times were performed as described previously.[41−43] Total fluorescence quantum yields were measured relative to BBOT (2,5-bis-(5-*tert*-butyl-2-benzoxazolyl)thiophene) as a standard, and absolute fluorescence quantum yields were calculated according to the following formula:[43]

$$Q_F(\mathrm{BA}) = Q_F(\mathrm{BBOT})\frac{I(\mathrm{BA})}{I(\mathrm{BBOT})}\frac{n_{sol}^2(\mathrm{BA})}{n_{sol}^2(\mathrm{BBOT})}$$

Herein, I is the integrated fluorescence intensity and n_{sol} the refractive index of the solvent used. $Q_F = 0.74$ was used for BBOT in cyclohexane.[44,45] Slit widths, amplification factors, and excitation wavelength (370 nm) were the same for all measurements. The optical density of the solutions was 0.16 ± 0.01.

The third harmonic ($\lambda = 355$ nm) of a Q-switched Nd:YAG laser (Quanta-Ray DCR-1, pulse length of 10 ns) was used for excitation in the nanosecond time-resolved experiments. Transient absorption was measured in a right-angle geometry using

a 450 W xenon arc, a high-intensity monochromator (Schoeffel Kratos), a Hamamatsu R3896 photomultiplier, and a digitizing scope (Tektronix TDS 684A). Stray light on the photomultiplier due to BA fluorescence was minimized by putting a solution of $NiSO_4$ and/or $CoSO_4$ between cell and monochromator.

A variant of the traditional energy-transfer method[46] was employed for the experimental determination of the intersystem-crossing quantum yield Q_{ISC} of BA in the solvents isooctane, ethanol, and acetonitrile. Since anthracene cannot be used as the acceptor for energy transfer from triplet BA, naphthacene was selected for this purpose on the grounds of its distinctly lower triplet energy (1.3 eV compared to 1.8 eV for anthracene[47]). An intense triplet−triplet transition with a maximum around 465 nm ($\epsilon^{465} = 3120$ m^2 mol^{-1}) has been recorded for naphthacene in benzene.[48] We redetermined the triplet−triplet spectrum of naphthacene by direct excitation at $\lambda_{exc} =$ 266 nm in isooctane and acetonitrile and found in both solvents a spectrum with three bands characterized by maxima at 429, 456, and 473 nm, the most intense band being that at 456 nm; ground-state absorption is small at this wavelength, resulting in a correction factor for ground-state depletion of less than 5%. The problem of the unknown Q_{ISC} of naphthacene (a value of 0.62 for a solution in benzene is available from the literature,[49] but our own data indicated a marked solvent dependence) was circumvented by using, respectively, anthracene and BA as donors in two separate experiments at $\lambda_{exc} = 355$ nm. At this wavelength, the absorption of naphthacene is negligible. Energy transfer from anthracene or BA to naphthacene took place as evidenced by the buildup of the naphthacene triplet−triplet spectrum. Combining both measurements allowed the determination of Q_{ISC} of BA based on $Q_{ISC} = 0.7$ for anthracene.[49]

2.4. Semiempirical Calculations. Semiempirical calculations were carried out using the AM1 Hamiltonian as implemented in the VAMP 6.0 program (Oxford Molecular Ltd.).[50] BA was optimized in the ground state, and vertical spectra were calculated using a CI procedure in which only the single and pairwise double excitations between the six highest occupied and six lowest unoccupied orbitals are included. This PECI method gives good results for electronic spectra, and transition dipoles can also be calculated. Excellent agreement has been noted[51] between calculated electronic spectra of organic molecules and experimental data, both regarding spectral positions and oscillator strengths. Solvent effects were accounted for by single-point calculations using the numerical self-consistent reaction-field method recently described by Rauhut and Clark.[52]

3. Results and Discussion

3.1. UV−Vis Absorption Spectra. Absorption spectra of BA were measured in the range of solvents as given in the Experimental Section. The spectral position of the BA absorption maximum does not depend on the solvent polarity, i.e., the static dielectric constant D, but is a function of solvent polarizability. It is proportional to $(n^2 - 1)/(n^2 + 2)$ and varies between 25 870 cm^{-1} in 2,2,2-trifluoroethanol ($n_D^{293} = 1.291$) and 25 030 cm^{-1} in carbon disulfide ($n_D^{293} = 1.626$). This behavior indicates that the interaction energy of excited and ground-state BA with the solvent molecular environment is dominated by contributions due to dispersive forces. The red shift of the absorption of BA with respect to that of anthracene (920 cm^{-1} in isooctane) and the significant increase of the absorption intensity (the integral over the first absorption band is 6.34×10^8 m mol^{-1} for BA but 2.23×10^8 m mol^{-1} for an isolated anthracene unit) indicate weak conjugation between the orbitals centered on the two anthracene moieties and/or resonance between the two involved absorption transitions.

TABLE 1: Fluorescence Quantum Yields, Spectral Emission Maxima, Fluorescence Lifetimes, and Rate Constants of Radiative Deactivation of 9,9′-Bianthryl in Several Solvents

	solvent	Q_F	$\tilde{\nu}_F$ cm^{-1}	τ_F ns	k_F 10^7 s^{-1}
1	isooctane	0.65 ± 0.03	24 200	7.43	8.7
2	benzene	0.95 ± 0.04	23 700	10.61	9.0
3	toluene	0.75 ± 0.01	23 800	10.66	7.0
4	tetralin	0.81 ± 0.02	23 800	10.18	8.0
7	tetrachloromethane	0.10 ± 0.01	23 900		
8	1,2-dichloroethane	0.54 ± 0.04	22 100	32.46	1.7
11	1-chlorobutane	0.67 ± 0.03	23 900	13.43	5.0
12	chlorobenzene	0.87 ± 0.02	22 800	15.48	5.6
15	ethyl ether	0.62 ± 0.01	24 000	13.84	4.5
16	*tert*-butyl methyl ether	0.64 ± 0.02	24 100	12.43	5.1
18	butyl ether	0.62 ± 0.01	24 000	10.21	6.1
19	tetrahydrofuran	0.61 ± 0.02	22 800	21.33	2.9
21	butanone	0.36 ± 0.01	22 200	27.35	1.3
22	cyclohexanone	0.57 ± 0.01	22 300	25.85	2.2
27	acetonitrile	0.33 ± 0.01	20 900	35.26	0.94
31	*N*-methylpyrrolidone	0.55 ± 0.02	21 200	42.74	1.3
35	methanol	0.45 ± 0.02	21 600	33.89	1.3
36	ethanol	0.53 ± 0.01	22 300	29.41	1.8
37	2,2,2-trifluoroethanol	0.08 ± 0.01	20 100	16.00	0.50

3.2. Fluorescence Properties. *3.2.1. General Features.* Fluorescence properties of BA were measured in a wide variety of solvents (more than 50) in order to obtain spectral and kinetic data over the whole range of solvent polarity. This approach affords the possibility of discerning solvent effects arising from bulk properties from specific effects of individual solvents. This is of particular concern in the low-polarity range, since the onset of intramolecular charge-transfer relaxation is expected there but specific solute−solvent interactions will be more important than at high polarities.

3.2.2. Fluorescence Spectra and Quantum Yields. The fluorescence spectra of BA in fluid solution change strongly in shape and position when a hydrocarbon solvent is replaced by polar solvents. This spectral behavior was the subject of several studies.[8,14,15] Fluorescence is generally viewed to be composed of two bands, one originating from a nondipolar, nonplanar excited state and a second one from a highly dipolar charge-transfer state.[29] The two emissions overlap strongly, and no significant broadening of the spectra is observed; spectral decomposition has to be used to separate the contributions of both emissions to the composite band. In solvents of low polarity ($f(D) = (D - 1)/(D + 2) < 0.5$), the shift of the fluorescence maximum is rather small and fluorescence thus predominantly originates from the nonpolar state. The relative shift increases sharply at higher polarities, and emission from the charge-transfer state is mainly observed in these solvents.

The fluorescence properties (absolute quantum yields, spectral position of maximum emission, lifetimes, and rate constants of radiative deactivation) of BA in some selected solvents are collected in Table 1.

The fluorescence quantum yields are strongly solvent-dependent but do not correlate with solvent polarity. Q_F may slightly decrease as the polarity increases, but this trend, if real, is buried in a large scatter reflecting other influences, such as specific solute−solvent interactions or heavy atom quenching. The fluorescence yields are low in triethylamine, a good electron donor, and in carbon disulfide, a good acceptor, as well as in solvents containing bromine or iodine atoms. Benzene represents a special case too, since in this solvent Q_F is considerably higher than in similar nonpolar solvents.

3.2.3. Fluorescence Lifetimes. In contrast to the irregular solvent-dependence behavior of the fluorescence quantum yields, the experimental fluorescence lifetimes τ_F increase steadily with

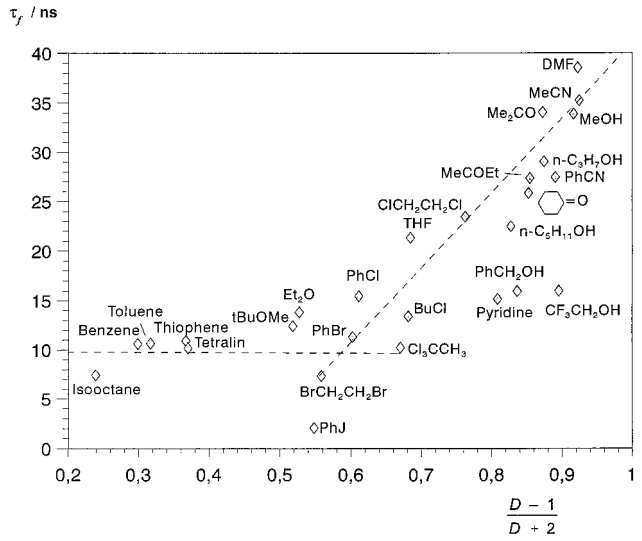

Figure 1. Fluorescence lifetime τ_F of 9,9′-bianthryl in various solvents as a function of the polarity function $(D - 1)/(D + 2)$.

increasing solvent polarity but only in solvents whose dielectric constant exceeds a value of $D = 5$. In solvents of lower polarity, τ_F scatters about a value of about 8 ns, most likely owing to local solute−solvent interactions, but on average is independent of the bulk dielectric constant. However, as D exceeds 5.5 (i.e., when the polarity function $f(D)$ becomes larger than 0.6), the fluorescence lifetime increases rapidly and reaches a maximum value of almost 43 ns in highly polar amides (see Figure 1). The scatter of these values about an interpolating function is much less significant than for Q_F if one excludes those solvents where the influence of a specific solute−solvent interaction is again clearly indicated. This applies in particular to tetrachloromethane, which features a double-exponential fluorescence decay. The lifetime measured in benzene solution fits excellently to that of similar nonpolar solvents, although the quantum yield is extraordinarily high. Consequently, the nonradiative decay rate constant is very small in this solvent.

Two distinct polarity regions are thus coined by strongly different solvent effects on the fluorescence lifetime. As shown by the solvent dependence of the emission maximum (Figure 2a), the fluorescence spectra behave in a similar way. In contrast, this does not hold for the radiative decay rate constants k_F. Their values, as calculated from Q_F and τ_F, decrease nearly linearly with increasing polarity (Figure 2b). Correcting for the influence of refractive index variations or of the shift of the fluorescence spectrum reduces the scatter of the k_F values about an interpolating function but does not change the quasi-linear relationship.

It is instructive to compare the experimental values of k_F to the natural decay times calculated from the absorption spectra according to the Strickler−Berg equation.[53] In isooctane, $\tau_{F,calc}^{\circ} = 6.1$ ns ($k_F = 16.4 \times 10^7$ s^{-1}) is obtained. The experimental value is $\tau_{F,exp}^{\circ} = 8.7$ ns ($k_F = 11.5 \times 10^7$ s^{-1}). In methanol, on the other hand, $\tau_{F,calc}^{\circ} = 8.9$ ns ($k_F = 11.2 \times 10^7$ s^{-1}) is much smaller than the experimental value $\tau_{F,exp}^{\circ} = 77$ ns ($k_F = 1.3 \times 10^7$ s^{-1}). A small rate constant is generally held to indicate the occurrence of radiative back electron transfer; this is emphasized by the large value of $\tau_{F,exp}^{\circ}$ in polar solvents. However, the discrepancy between experimental and calculated radiative lifetimes is already substantial in hydrocarbon solutions, indicating either a significant change in excited-state geometry or significant contributions from a charge-transfer state to the emission even at low polarities. Which of the two

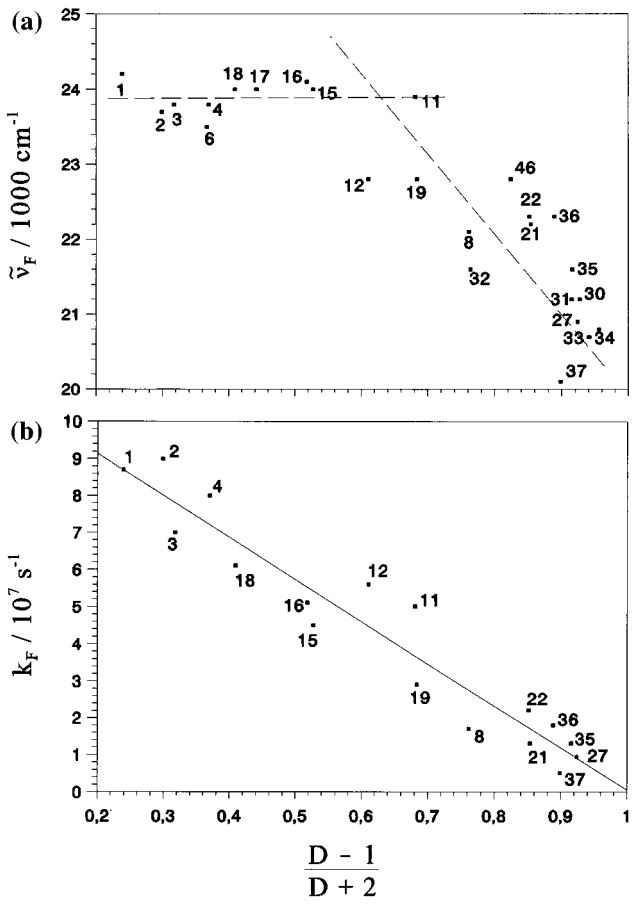

Figure 2. Maximum $\tilde{\nu}_F$ of the fluorescence band (a) and rate constant k_F of fluorescence (b) of 9,9′-bianthryl in various solvents as a function of their polarity given by $(D - 1)/(D + 2)$.

possibilities applies can hardly be decided from the fluorescence data alone. From the discussion given below, it will become obvious that the second possibility can be ruled out. This conclusion will be based on the fact that no indication of an intramolecular charge-separated state is found in the singlet−singlet absorption spectra in nonpolar solution, and on the results of semiempirical calculations that locate this state, in a hydrocarbon environment, far above a relaxed nonpolar excited state with a geometry where the anthracene moieties are no longer perpendicular to each other. The contributions from a charge-separated asymmetric state thus being unlikely in hydrocarbons, an alternative model incorporating structural relaxation must be favored, such as that proposed by Wortmann et al.[15, 27] based on planarization in a nondipolar state. The continuous decrease of the radiative rate constant with increasing solvent polarity is thus most likely due to contributions from two different mechanisms: structural relaxation at lower polarities and charge-transfer at higher ones.

3.3. Singlet−Singlet ($S_n \leftarrow S_1$) Absorption. In polar solvents, such as acetonitrile, ethanol, or *N*-methylpyrrolidone, a strong short-lived transient with a maximum at 315 nm is detected immediately after excitation of BA with a laser pulse of 10 ns duration at $\lambda_{exc} = 355$ nm (Figure 3, spectrum 1). In the nonpolar solvent isooctane, this band is absent and a much weaker absorption increasing toward longer wavelengths ($\lambda_{max} > 350$ nm) is observed (Figure 3, spectrum 3).

The time courses of the transient absorption as measured at 315 nm in acetonitrile and isooctane are displayed in Figure 4.

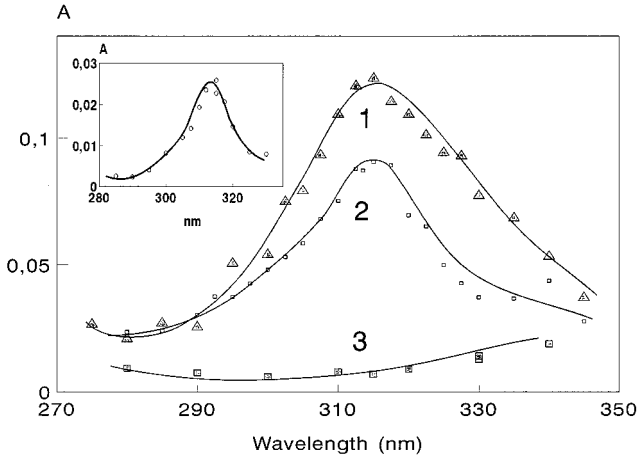

Figure 3. Transient-absorption spectra obtained by laser-pulse excitation of BA (5×10^{-5} M) (1) in CH_3CN measured at pulse end (0.38 mJ/pulse), (2) in O_2-saturated CH_3CN measured 200 ns after pulse end (6.7 mJ/pulse), (3) in isooctane measured at pulse end (0.38 mJ/pulse). The insert shows the absorption spectrum of the radical cation of anthracene in ethanol (7.2 mJ/pulse).

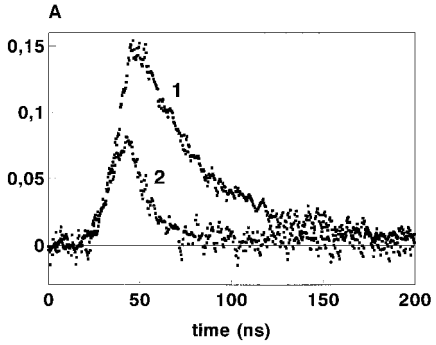

Figure 4. Time course of laser-pulse-induced BA transients: (1) in CH_3CN, 315 nm, 0.48 mJ/pulse; (2) in isooctane, 330 nm, 1.8 mJ/pulse.

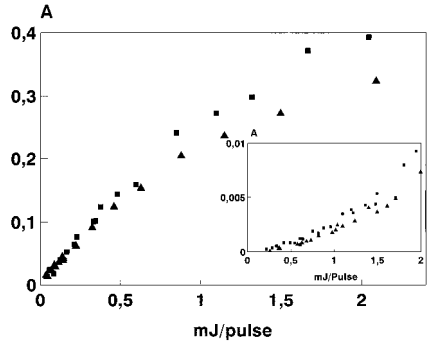

Figure 5. Dependence of laser-pulse-induced transient absorbance of BA in CH_3CN on laser pulse energy: (■) $\lambda = 315$ nm measured at pulse end; (▲) $\lambda = 425$ nm measured 200 ns after pulse end and absorbances multiplied by factor of 2. The insert shows that of BA (5×10^{-5} M) in ethanol: (■) argon-saturated solution, $\lambda = 700$ nm, measured at pulse end; (▲) O_2-saturated solution, $\lambda = 315$ nm, measured 1 μs after pulse end.

Kinetic analysis shows that these transients decay by first-order reactions. The decay is distinctly faster in isooctane than in acetonitrile.

The dependence of the transient absorbance at pulse end, measured at 315 nm for BA in acetonitrile, on the laser pulse energy is shown in Figure 5 along with the absorbance of the triplet−triplet band at 425 nm (see below). Both series of data exhibit an initially linear dependence on pulse energy, with beginning saturation at higher energies. This behavior indicates transient formation by one-photon processes.

TABLE 2: $S_n \leftarrow S_1$ Absorption of BA in Various Solvents and Comparison with Fluorescence Decay

	solvents	ϵ^{315} $m^2\ mol^{-1}$	k_{decay} s^{-1}	$(1/k_{decay})$ ns	τ_F ns
1	isooctane		$>10^8$	<10	7.43
12	chlorobenzene	~1000	6.0×10^7	16.7	15.48
19	tetrahydrofuran	1560	4.45×10^7	22.5	21.33
27	acetonitrile	2420	2.95×10^7	34.0	35.26
31	NMP	2350	2.3×10^7	43.5	42.74
36	ethanol	1900	3.8×10^7	26.3	29.41

Table 2 shows the spectral and kinetic characteristics of the 315 nm transient in a series of solvents and compares the lifetimes ($1/k_{decay}$) with the fluorescence lifetimes. In all solvents studied with the exception of isooctane, where the transient decay rate was too high to be determined, there is excellent agreement between both parameters. This strongly suggests the assignment of the 315 nm band to the singlet−singlet ($S_n \leftarrow S_1$) absorption of BA.

The characterization of $S_n \leftarrow S_1$ absorption in polar solvents is aided by comparison with the spectra of radical ions of BA. Figure 3 (spectrum 2) shows the spectrum of the radical cation of BA obtained by laser-pulse-induced two-photon ionization in an O_2-saturated solution in ethanol, measured after decay of the much shorter-lived $S_n \leftarrow S_1$ absorption. The assignment of this band to the BA radical cation is based on the observation that its dependence on laser pulse energy parallels that of the simultaneously formed solvated electrons monitored by their absorption at 700 nm in argon-saturated solution (see insert in Figure 5). Both transients show a markedly nonlinear (parabolic) dependence on pulse energy as expected for the products of a two-photon excitation process. An extinction coefficient $\epsilon^{315} = 1400\ m^2\ mol^{-1}$ can be estimated with reference to $\epsilon^{700} = 1800\ m^2\ mol^{-1}$ for the solvated electron.[54] A further comparison can be made with the spectrum of the radical cation of anthracene, displayed in the insert of Figure 3. $\epsilon^{315} = 1800\ m^2 mol^{-1}$ is determined for this species, using again ethanol as a solvent. The similarity of the two spectra is indicative of localization of the unpaired spin of the BA radical cation on one anthracene moiety. A similar conclusion has been reached for electrochemically generated BA radical anions,[55] which also have a strong absorption band near 320 nm.

It is obvious from Figure 3 that the absorption spectra of the BA radical cation and that of the BA $S_n \leftarrow S_1$ transition in polar solvents are quite similar; the band maximum lies at 315 nm in both cases, although the $S_n \leftarrow S_1$ band is somewhat broader. The extinction coefficients of the latter appears to be significantly higher than that of the radical cation: a value $\epsilon^{315} \approx 2100\ m^2\ mol^{-1}$ is deduced from the data in Table 2 for the $S_n \leftarrow S_1$ transition of BA, assuming $Q(S_n \leftarrow S_1) = 1$. These observations indicate that this transition is equivalent to the overlapping absorptions of a radical cation and a radical anion of anthracene, as expected for a fully charge-separated state.

The present results thus corroborate those of previous studies,[34−36] which attributed the transient observed by picosecond absorption spectroscopy in polar solvents to the charge-separated fluorescing state, and for the first time provide direct proof of this attribution by virtue of the equality of the transient lifetimes with the fluorescence lifetimes in various solvents.

In contrast, the $S_n \leftarrow S_1$ absorption of BA in isooctane (Figure 3) is characterized by a minimum around 300 nm. The spectral increase toward longer wavelengths is in agreement with literature data on the $S_n \leftarrow S_1$ absorption of anthracene.[56] It

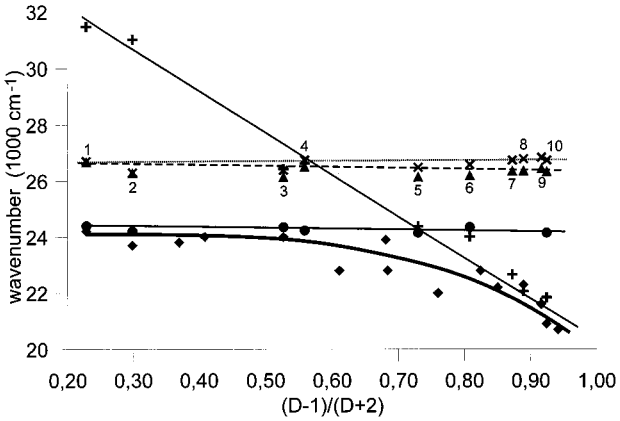

Figure 6. Transition energies resulting from semiempirical calculations on orthogonal BA of D_{2d} symmetry ((× and dotted line) vertical absorption; (▲ and broken line) fluorescence of vertically excited state; (+ and full line) fluorescence from charge-separated state) and of BA of D_2 symmetry for a torsion angle of 67° ((● and full line) fluorescence). Absorption energies are calculated for a nonrelaxed solvent cage and fluorescence energies for a fully relaxed solvent cage. Experimentally determined fluorescence maxima are also shown (◆ and full line). Solvents used are (1) hexane, (2) benzene, (3) diethyl ether, (4) chloroform, (5) methylene chloride, (6) acetone, (7) ethanol, (8) pyridine, (9) methanol, and (10) acetonitrile.

becomes clear from Figures 3 and 4 that a possible contribution of a charge-transfer state to the $S_n \leftarrow S_1$ absorption in isooctane cannot amount to more than 5% of its absorption in acetonitrile. The present study therefore does not confirm previous reports of a substantial charge-transfer character of the S_1 state in nonpolar solvents.[4,29]

3.4. Semiempirical Calculations. Given the lack of experimental evidence of charge separation in the fluorescent state in nonpolar solvents, the question now arises whether this result can be understood theoretically. Semiempirical calculations have been performed to this effect.

BA was restricted to D_{2d} symmetry for minimization in the ground state, i.e., the two anthracene subunits were kept planar and fully symmetric and the respective torsion angle was set to 90°. The two highest occupied as well as the two highest unoccupied orbitals are degenerate (symmetry species e). This leads to four excited states: the symmetric and antisymmetric combinations of the two local excitations on the two subunits and the two "charge-transfer transitions" (CT) between the highest occupied and lowest unoccupied orbitals centered on different moieties. The lowest excited state is of B_2 symmetry (arising from the antisymmetric combination of the two local excitations), and excitation into this state represents the only allowed transition. In the gas phase, the energy of this state is 3.249 eV (26 200 cm^{-1}, 382.6 nm) above the ground state. The oscillator strength is 0.437, and the transition is polarized along the bond connecting the two subunits. This oscillator strength may be compared to the value of 0.103 found for anthracene under comparable conditions. The S_2 state, corresponding to the symmetric combination of the CT transitions, is found at 3.539 eV (28 550 cm^{-1}, 350.3 nm) above the ground state. The two other states arising from the excitation of the two degenerate orbitals appear as S_5 and S_6 and correlate with the antisymmetric CT and the symmetric combination of local excitations, respectively, and are found at 4.180 eV (33 710 cm^{-1}, 296.6 nm) and at 4.347 eV (35 060 cm^{-1}, 285.2 nm). The permanent dipole moment is zero for all these states. The sequence of states and the oscillator strengths are strongly affected by subtle deviations from D_{2d} symmetry. Both the position of the absorption maximum as well as the oscillator strength relative to anthracene are in good agreement with the experimental results reported above.

Torsion about the single bond connecting the two subunits causes a reduction of D_{2d} symmetry to D_2, a nondegenerate point group. From molecular-jet experiments and the simulation of the fluorescence spectrum in nonpolar solvents, it has been concluded[24−27] that the torsional angle in the fluorescent S_1 state in nonpolar solvents is not 90° but rather near 70°. Assuming a value of 70° for the torsion angle, the S_1 energy of symmetric BA (D_2 symmetry) decreases by 1.51 kJ mol^{-1} in comparison to the perpendicular geometry, whereas the ground-state energy increases by 7.9 kJ mol^{-1}. The former value is lower than that experimentally determined in supersonic-jet measurements.[26] The discrepancy may be due to the fact that the calculations are based on Franck−Condon geometries, neglecting other possible relaxation pathways such as bond-length changes in the anthracene subunits. Torsional motion thus induces both stabilization of the excited state and destabilization of the ground state, resulting in a fluorescence shift.

Energies of absorption and fluorescence and the effects of solvation on these energies were calculated for ground and excited states assuming a fully relaxed solvent cage in each state. The applied model uses an arbitrarily shaped van der Waals cavity. The total free energy contains the electrostatic and dispersive contributions as well as the free cavity energy. Two degenerate excited states with large dipole moments (67.1 × 10^{-30} C m) are obtained as S_5 and S_6 for perpendicular BA (D_{2d}) in hexane in a fully relaxed solvent cavity. They correspond to the two charge-transfer transitions, which are discernible because of different orientations of the solvent dipoles. The corresponding fluorescence energy shifts strongly bathochromically as the solvent becomes more polar. This behavior is only obtained in the perpendicular geometry.

The transition energies for the vertical excitation $S_1(D_{2d}) \rightarrow S_0$ and $S_5(D_{2d}) \rightarrow S_0$ fluorescence transitions of perpendicular BA (D_{2d}), and for the $S_1(D_2) \rightarrow S_0$ fluorescence transition of BA (D_2) with a torsion angle of 70° were calculated for 10 different solvents. The results are shown in Figure 6. In a nonrigid and nonpolar medium the twisted $S_1(D_2)$ state is the lowest excited state. The $S_1(D_2) \rightarrow S_0$ fluorescence is shifted to lower energies by 1200 cm^{-1} when compared to fluorescence originating from the vertically excited $S_1(D_{2d})$ state. Both states are nonpolar, and solvent shifts are therefore small. The S_5-(D_{2d}) charge-transfer state, which lies distinctly higher in a nonpolar environment, is strongly stabilized by a polar solvent, and emission from this state becomes the lowest fluorescence transition as the solvent polarity function $f(D)$ exceeds 0.7.

The experimental fluorescence band maxima are plotted in Figure 6 for comparison. It is obvious that they follow closely the solvent-polarity dependence proposed by the semiempirical calculations. It can be concluded that a twisted nonpolar state is the main fluorescent state in low-polarity solvents, whereas the charge-separated state becomes the lowest state and predominates over emission in solvents of higher polarity. Since the charge-separated state lies approximately 4000 cm^{-1} above the lowest excited singlet state in hydrocarbon solvents, it seems unlikely that it could be populated to any significant amount in a nonpolar environment.

3.5. Triplet−Triplet ($T_n \leftarrow T_1$) Absorption and Intersystem-Crossing Yields. Earlier studies on the triplet−triplet absorption of BA noted its similarity to that of anthracene and its insensitivity to solvent, as opposed to the behavior of the singlet−singlet absorption.[34,38] In the following, we present the results of a more detailed and quantitative study.

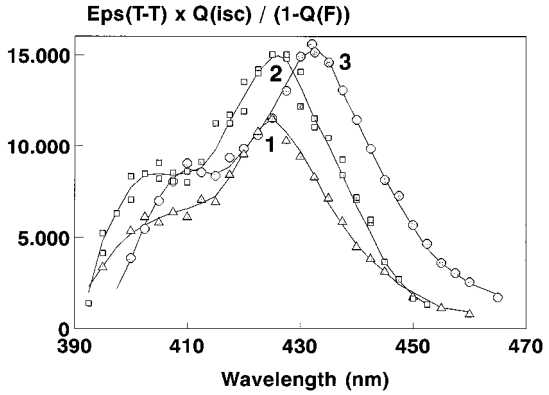

Figure 7. Triplet−triplet absorption spectra of BA in ethanol (1), isooctane (2), and *N*-methylpyrrolidone (3).

TABLE 3: Triplet Properties of BA in Various Solvents and Comparison with Fluorescence Quantum Yields

	solvent	λ_{max} nm	$\Delta\lambda_{1/2}$ nm	$\epsilon Q(\lambda\text{max})$ $m^2\ mol^{-1}$	Q_{ISC}	$1 - Q_F$	k_{ISC} $10^6\ s^{-1}$
1	isooctane	426	27	540	0.30[a]	0.35	41
2	benzene	436	29.5	99	0.06[b]	0.05	5.7
7	tetrachloromethane	427	54	109	0.12[b]	0.90	
12	chlorobenzene	432.5	32.5	210	0.14[b]	0.13	9.1
19	tetrahydrofuran	427.5	22	285	0.13[b]	0.39	9.4
22	cyclohexanone	428	24.5	400	0.20[b]	0.43	13
27	acetonitrile	426	24	1150	0.54[a]	0.67	16
31	NMP	432.5	26	697	0.37[b]	0.45	8.7
35	methanol	426	28	605	0.56[c]	0.55	17
36	ethanol	426	25	547	0.42[a]	0.47	16
37	2,2,2-trifluoroethanol	423	24.5	1030	0.84[c]	0.92	53

[a] Measured by means of energy transfer to naphthacene (see text). [b] Calculated by using Q_{ISC} in isooctane as a reference value and assuming oscillator strength of T−T transition to be solvent-independent. [c] Same as footnote b but assuming oscillator strength reduced by a factor 0.6 compared to the oscillator strength in isooctane.

In all solvents studied, a transient with a maximum in the 425−430 nm range was detected upon irradiation of BA (λ_{exc} = 355 nm) with 10-ns laser pulses (Figure 7). This transient was quenched by oxygen and assigned to a triplet−triplet absorption, in agreement with earlier measurements.[38] Its pulse energy dependence is initially linear and parallels that of the $S_n \leftarrow S_1$ absorption (Figure 5), in support of the assignment.

Spectral and pulse-energy-dependent measurements of the triplet−triplet absorption have been carried out in a number of solvents. The main results are collected in Table 3. The spectral half-widths have been determined by Gaussian fits of the main absorption band. Values of intersystem-crossing quantum yield (Q_{ISC}) times the triplet−triplet extinction coefficient are obtained from the initial slope of the pulse-energy-dependent transient absorbance plots, such as that shown in Figure 5. Q_{ISC} values in the solvents isooctane, ethanol, and acetonitrile were determined by energy transfer to naphthacene as described in the Experimental Section. Q_{ISC} values in other solvents were determined from $\epsilon Q(\lambda_{max})$ values assuming a triplet−triplet oscillator strength f(T−T) identical with that determined in isooctane, with the exception of methanol and 2,2,2-trifluoroethanol for which f(T−T) was reduced by a factor of 0.6 (see below).

The intersystem-crossing yields of BA thus determined are in reasonable agreement with those available from the literature.[29,38] Comparison with the values of $1 - Q_F$ indicates that in most solvents the quantum yields of fluorescence and intersystem crossing add to unity or nearly so, as suggested previously.[29] Cyclohexanone, tetrahydrofuran, and, in a most pronounced way, tetrachloromethane are exceptions from this rule, indicating that in these solvents radiationless deactivation pathways may be induced by specific solute−solvent interactions.

The data of Table 3 corroborate the conclusion of previous studies[34,38] according to which BA triplet−triplet absorption is much less solvent-dependent than fluorescence emission and does not show the characteristics of charge separation. Solvent influence on the triplet−triplet absorption is not entirely absent, however, and indeed, there seem to be some features that are specific for the BA triplet state. This can be concluded from the following observations.

(1) The band maximum is solvent-dependent. Although it is true that a weak solvent dependence is also noted in the ground-state absorption spectra, the effect is much more pronounced in the triplet−triplet absorption.

(2) The same is true for the band half-widths. In this respect, it is also significant that the triplet−triplet band of BA is much broader than that of anthracene ($\Delta\lambda_{1/2}$ = 8 nm for anthracene in hexane[46]), the oscillator strengths as calculated from the spectra being comparable in magnitude (f = 0.11 for BA and 0.13 for anthracene in alkane solvents). The difference between the ground-state absorption band half-widths is much less pronounced; the half-width of the 0−0 band in isooctane is 5 nm for anthracene and 8 nm for BA.

(3) A particular behavior of the BA triplet−triplet absorption is seen when alcohols are used as solvents. Figure 7 shows the triplet−triplet spectra in ethanol, isooctane, and *N*-methylpyrrolidone (NMP). In this figure, the abscissa has been expressed as the T−T extinction coefficient scaled by the factor $Q_{ISC}/(1 - Q_F)$. The spectrum in NMP is red-shifted with respect to that in isooctane as noted above. In contrast, the spectrum in ethanol does not show a spectral shift but is distinctly weaker. The same behavior was noted when methanol or 2,2,2-trifluoroethanol was used as solvents. Since $Q_{ISC} \approx (1 - Q_F)$ both in isooctane and ethanol (Table 3), it must be concluded that triplet−triplet oscillator strengths are systematically lower in the alcohols. If this effect is taken into account in the estimation of Q_{ISC}, $Q_{ISC} \approx (1 - Q_F)$ holds also in methanol and 2,2,2-trifluoroethanol (see Table 3). It should be noted here that differences between alkanols and other solvents have earlier been recorded in measurements of fluorescence solvatochromy[8,57] and attributed to specific solute−solvent interactions.[8]

(4) The values of the intersystem-crossing rate constant k_{ISC} show large variations among different solvents (Table 3). This behavior has been explained[29] by assuming triplet population from both locally excited and charge-transfer singlet states, with this latter step being solvent-dependent. The data shown in Table 3 are hard to reconcile with this picture, since variations of k_{ISC} within groups of solvents of comparable polarity (isooctane/benzene on one hand, *N*-methylpyrrolidone/ethanol/2,2,2-trifluoroethanol on the other) appear to be considerably larger than any systematic polarity-dependent trend. Again, it must be concluded that specific solvent−solute interactions are essential in determining the intersystem-crossing kinetics of BA.

Conclusions

A consistent picture of the solvent dependence of 9,9′-bianthryl photophysics emerges from the results of this study, whose central feature is the existence of two distinct deactivation pathways prevailing in the domains of low and high solvent polarity, respectively. This picture is based on new experimental data obtained by fluorescence and transient-absorption spectroscopy. Singlet−singlet absorption provides for the first time

SCHEME 2

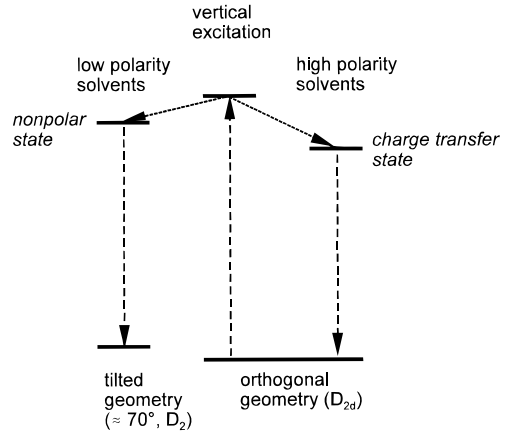

direct evidence for charge separation in polar solvents by virtue of the equality of the measured decay kinetics with those of fluorescence decay and shows that there is no substantial charge separation in a nonpolar environment. The investigation of fluorescence characteristics in a large number of solvents allows the experimental establishment of a quasi-continuous function that shows that in the region of small polarities ($D < 5$) there is no *unspecific* dependence on bulk-solvent polarity. In several solvents, fluorescence as well as triplet−triplet absorption show, however, the marks of *specific* solute−solvent interactions that doubtless are due to the high polarizability of the BA molecule.

Careful consideration of the symmetry properties of the molecular states involved, as well as of solvent influences on these states, allows a rationalization of these results. The resulting new picture of the photophysics of 9,9′-bianthryl is qualitatively summarized in Scheme 2. In nonpolar solvents, the observed fluorescence should correspond to a $S_1(D_2) \rightarrow S_0$ transition from a nonpolar excited state with a torsion angle of distinctly less than 90° between the anthracene moieties. In polar solvents, on the other hand, a perpendicular charge-separated singlet state of D_{2d} symmetry is the lowest excited state. The influence of solvent polarity on this state accounts for the large effect of solvent polarity on fluorescence parameters. In summary, dual fluorescence is due to the existence of two emitting states, a solvent-dependent one and a solvent-independent one, which are unable to interconvert thermally except in a very limited range of solvent polarities.

Acknowledgment. Financial support by the Fonds zur Förderung der wissenschaftlichen Forschung in Österreich (Project No. P11880-CHE) is gratefully acknowledged.

References and Notes

(1) Rettig, W. *Angew. Chem., Int. Ed. Engl.* **1986**, *25*, 971.
(2) Rotkiewicz, K.; Grellmann, K. H.; Grabowski, Z. R. *Chem. Phys. Lett.* **1973**, *19*, 315; **1973**, *21*, 212 (erratum).
(3) Grabowski, Z. R.; Rotkiewicz, K.; Siemiarczuk, A.; Cowley, D. J.; Baumann, W. *Nouv. J. Chim.* **1979**, *3*, 443.
(4) Visser, R. J.; Weisenborn, P. C. M.; van Kan, J. M.; Huizer, B. H.; Varma, C. A. G. O.; Warman, J. M.; de Haas, M. P. *J. Chem. Soc., Faraday Trans.* **1985**, *81*, 689.
(5) Beens, H.; Weller, A. *Chem. Phys. Lett.* **1969**, *3*, 666.
(6) Schneider, F.; Lippert, E. *Ber. Bunsen-Ges. Phys. Chem.* **1968**, *72*, 1155.
(7) Baumann, W.; Spohr, E.; Bischof, H.; Liptay, W. *J. Lumin.* **1987**, *37*, 227.
(8) Rettig, W.; Zander, M. *Ber. Bunsen-Ges. Phys. Chem.* **1983**, *87*, 1143.
(9) Lippert, E.; Rettig W.; Bonačić-Koutecký, V.; Heisel, F.; Miehé, A. J. *Adv. Chem. Phys.* **1987**, *68*, 1.
(10) Anthon, D. W.; Clark, J. H. *J. Phys. Chem.* **1987**, *91*, 3530.
(11) Kang, T. J.; Jarzęba, W.; Barbara, P. F.; Fonseca, T. *Chem. Phys.* **1990**, *149*, 81.
(12) Barbara, P. F.; Jarzęba W. *Adv. Photochem.* **1990**, *15*, 1.
(13) Tominaga, K.; Walker, G. C.; Kang, T. J.; Barbara, P. F.; Fonseca, T. *J. Phys. Chem.* **1991**, *95*, 10485.
(14) Müller, S.; Heinze, J. *Chem. Phys.* **1991**, *157*, 231.
(15) Wortmann, R.; Lebus, S.; Elich, K.; Assar, S.; Detzer, N.; Liptay, W. *Chem. Phys. Lett.* **1992**, *198*, 220.
(16) Smith, M. J.; Krogh-Jespersen, K.; Levy, R. M. *Chem. Phys.* **1993**, *171*, 97.
(17) Dobkowski, J.; Grabowski, Z. R.; Paeplow, B.; Rettig, W.; Koch, K. H.; Müllen, K.; Lapouyade, R. *New J. Chem.* **1994**, *18*, 525.
(18) von der Haar, T.; Hebecker, A.; Il'ichev, Yu.; Jiang, Y.-B.; Kühnle, W.; Zachariasse, K. A. *Recl. Trav. Chim. Pays-Bas* **1995**, *114*, 430.
(19) Barbara, P. F.; Kang, T. J.; Jarzęba, W.; Fonseca, T. In *Perspectives in Photosynthesis*; Jortner, J., Pullman, B., Eds.; Kluwer: Dordrecht, 1990; p 273.
(20) Rettig, W. *Proc. Indian Acad. Sci., Chem. Sci.* **1992**, *104*, 89.
(21) Magnus, A.; Hartmann, H.; Becker, F. *Z. Phys. Chem.* **1951**, *197*, 75.
(22) Liptay, W.; Walz, G.; Baumann, W.; Schlosser, H.; Deckers, H.; Detzer, N. *Z. Naturforsch.* **1971**, *26a*, 2020.
(23) Hoijtink, J. *Recl. Trav. Chim. Pays-Bas* **1955**, *74*, 1525.
(24) Khundkar, L. R.; Zewail, A. H. *J. Chem. Phys.* **1986**, *84*, 1302.
(25) Yamasaki, K.; Arita, K.; Kajimoto, O.; Hara, K. *Chem. Phys. Lett.* **1986**, *123*, 24.
(26) Subaric-Leitis, A.; Monte, C.; Roggan, A.; Rettig, W.; Zimmermann, P.; Heinze, J. *J. Chem. Phys.* **1990**, *93*, 4543.
(27) Elich, K.; Kitazawa, M.; Okada, T.; Wortmann, R. *J. Phys. Chem. A* **1997**, *101*, 2010.
(28) Schneider, F.; Lippert, E. *Ber. Bunsen-Ges. Phys. Chem.* **1970**, *74*, 624.
(29) Schütz, M.; Schmidt, R. *J. Phys. Chem.* **1996**, *100*, 2012.
(30) Laguitton-Pasquier, H.; Pansu, R.; Chauvet, J.-P.; Collet, A.; Faure, J.; Lapouyade, R. *Chem. Phys.* **1996**, *212*, 437.
(31) Catalán, J.; Díaz, C.; López, V.; Pérez, P.; Claramunt, R. M. *J. Phys. Chem.* **1996**, *100*, 18392.
(32) Nagarajan, V.; Brearley, A. M.; Kang, T. J.; Barbara, P. F. *J. Chem. Phys.* **1987**, *86*, 3183.
(33) Honma, K.; Arita, K.; Yamasaki, K.; Kajimoto, O. *J. Chem. Phys.* **1991**, *94*, 3496.
(34) Nakashima, N.; Murakawa, M.; Mataga, N. *Bull. Chem. Soc. Jpn.* **1976**, *49*, 854.
(35) Mataga, N.; Yao, H.; Okada, T.; Rettig, W. *J. Phys. Chem.* **1989**, *93*, 3383.
(36) Lück, H.; Windsor, M.; Rettig, W. *J. Phys. Chem.* **1990**, *94*, 4550.
(37) Mataga, N.; Nishikawa, S.; Okada, T. *Chem. Phys. Lett.* **1996**, *257*, 327.
(38) Mac, M.; Najbar, J.; Wirz, J. *J. Photochem. Photobiol., A* **1995**, *88*, 93.
(39) Bell, F.; Waring, D. H. *J. Am. Chem. Soc.* **1949**, *71*, 267.
(40) *CRC Handbook of Chemistry and Physics*, 76th ed.; CRC Press: Boca Raton, FL, 1996.
(41) Köhler, G.; Rotkiewicz, K. *Spectrochim. Acta, Part A* **1986**, *42*, 1127.
(42) Köhler, G.; Wolschann, P. *J. Chem. Soc., Faraday Trans.* **1987**, *83*, 513.
(43) Birks, J. B. *Photophysics of Aromatic Molecules*; Wiley-Interscience: London, 1970; p 98. Rechthaler, K.; Köhler, G. *Chem. Phys. Lett.* **1996**, *250*, 152.
(44) Rechthaler, K.; Köhler, G. *Chem. Phys.* **1994**, *189*, 99.
(45) Berlman, I. B. *Handbook of Fluorescence Spectra of Aromatic Molecules*, 2nd ed.; Academic Press: New York, 1971; p 402.
(46) Bensasson, R.; Land, E. J. *Photochem. Photobiol. Rev.* **1978**, *3*, 163.
(47) Meyer, Y. H.; Astier, R.; Leclercq, J. M. *J. Chem. Phys.* **1972**, *56*, 801.
(48) Bensasson, R.; Land, E. J. *Trans. Faraday Soc.* **1971**, *67*, 1904.
(49) Amand, B.; Bensasson, R. *Chem. Phys. Lett.* **1975**, *34*, 44.
(50) Rauhut, G.; Alex, A.; Chandrashekar, J.; Clark, T. *VAMP 6.0*; Oxford Molecular Ltd.: Oxford, 1996.
(51) Clark, T.; Chandrasekhar, J. *Isr. J. Chem.* **1995**, *33*, 435.
(52) Rauhut, G.; Clark, T.; Steinke, T. *J. Am. Chem. Soc.* **1993**, *115*, 9174.
(53) Strickler, S. J.; Berg, R. A. *J. Chem. Phys.* **1962**, *37*, 814.
(54) Jou, F.-Y.; Freeman, G. R. *J. Phys. Chem.* **1979**, *83*, 2383.
(55) Grampp, G.; Kapturkiewicz, A.; Salbeck, J. *Chem. Phys.* **1994**, *187*, 391.
(56) Bebelaar, D. *Chem. Phys.* **1974**, *3*, 206.
(57) Kosower, E. M.; Tanizawa, K. *Chem. Phys. Lett.* **1972**, *16*, 419.